Effective operators in a single-j orbital

E Derbali, P. van Isacker, B. Tellili, C. Souga

Effective operators in a single-j orbital

E Derbali†, P Van Isacker‡, B Tellili§, and C Souga¶

† Unité de Recherche de Physique Nucléaire et des Hautes Energies, Faculté des Sciences de Tunis, Université de Tunis El-Manar, 2092 Tunis, Tunisia

‡ Grand Accélérateur National d'Ions Lourds, CEA/DRF–CNRS/IN2P3, Bvd Henri Becquerel, F-14076 Caen, France

§ Institut Superieur des Technologies Médicales de Tunis, Université de Tunis El-Manar, 1006 Tunis, Tunisia

¶ Ecole Polytechnique de Tunisie, Université de Carthage, B.P. 743-2078 La Marsa, Tunisia

Abstract. We present an analysis of effective operators in the shell model with up to three-body interactions in the Hamiltonian and two-body terms in electromagnetic transition operators when the nucleons are either neutrons or protons occupying a single-j orbital. We first show that evidence for an effective three-body interaction exists in the $N = 50$ isotones and in the lead isotopes but that the separate components of such interaction are difficult to obtain empirically. We then determine higher-order terms on more microscopic grounds. The starting point is a realistic two-body interaction in a large shell-model space together with a standard one-body transition operator, which, after restriction to the dominant orbital and with use of stationary perturbation theory, are transformed into effective versions with higher-order terms. An application is presented for the lead isotopes with neutrons in the $1g_{9/2}$ orbital.

1. Introduction

Three-body forces have become an accepted feature of the nuclear shell model [1]. They can be either real, arising because of the composite nature of the nucleon, or effective, induced by a renormalization to a given truncated model space. There is now considerable evidence for the existence of real three-body interactions in light nuclei [2] (see also the review [3]). Effective three-body interactions, on the other hand, are expected to occur in heavier nuclei since for such systems the effect of orbitals that are excluded because of model-space limitations can be important. If effective three-body interactions are included in the Hamiltonian, a consistent treatment requires effective higher-order corrections to other operators as well [4]. For electromagnetic transitions the usual approach is to introduce effective g factors or effective charges in the one-body operator (see, e.g. [5, 6]). However, one may question the use of a single effective g factor or effective charge, which can be state dependent. State-dependent renormalization can, in principle, be described by an effective two-body electromagnetic-transition operator but this is rarely done in shell-model calculations. (An exception is the two-body M1 operator of Ref. [7].)

In this paper we report on a study of effective Hamiltonians with up to three-body interactions and effective electromagnetic transition operators with up to two-body terms. For simplicity we limit ourselves to the manifestation of such higher-order corrections in nuclei with one kind of valence nucleon, and study the $T = 3/2$ three-body component of the nuclear interaction on top of its usual $T = 1$ two-body component. Therefore, our attention is focused on semi-magic nuclei with only nucleons of one kind, neutrons or protons, in the valence shell. The approach is further simplified by considering nuclei where the valence nucleons are dominantly in a single-j orbital.

While these are extreme simplifications of more realistic situations, this approach presents certain advantages. First of all, the shell-model calculations in the full space can be carried out for some of the nuclei that we consider here, thus enabling to check whether an expansion to a given order yields satisfactory results. Also, given the simplifying assumptions made, the perturbation method of Bloch and Horowitz [8] can be pushed to third order in the Hamiltonian and second order in the transition operators without an unwieldy proliferation of diagrams. Finally, for a single-j orbital the energy matrices are known analytically in terms of the interaction matrix elements, and calculations are easily carried out. In fact, it would be relatively straightforward to extend the current approach to test the performance of effective four-body interactions.

An early application of the shell model was the description of Ca isotopes ($Z = 20$) and $N = 28$ isotones with a two-body Hamiltonian in the $0f_{7/2}$ orbital [9, 10]. To improve results for binding energies and spectra, several authors considered, already many years ago, the inclusion of three-body interactions [11, 12]. In view of the current interest in three-body forces, the issue was revisited more recently by Volya [13], who studied the same semi-magic nuclei with a two-plus-three-body Hamiltonian. It was later shown [14] that the extracted three-body component can to some extent be understood as the result of excluded higher-lying orbitals, in particular $1p_{3/2}$. It the purpose of this paper (i) to present an application in the same spirit but to different nuclei, (ii) to extend perturbation theory for the effective two-plus-three-body Hamiltonian to third order, and (iii) to determine the effective one-plus-two-body transition operators to second order.

This paper is organized as follows. In Sect. 2 we define the Hamiltonian appropriate for identical nucleons in a single-j orbital. An effective single-j Hamiltonian with up to three-body interactions is derived in Sect. 3 and electromagnetic transition operators with up to two-body terms are derived in Sect. 4. With the recurrence relations for scalar and non-scalar k-body operators, as given in Sect. 5, we are then in a position to obtain all results, analytical if needed, in the context of a single-j orbital. In Sect. 6 we present the results of two applications, namely to the $N = 50$ isotones with protons in $0g_{9/2}$ and to the lead isotopes ($Z = 82$) with neutrons in $1g_{9/2}$. Finally, in Sect. 7 the conclusions of this study are summarized.

2. The single-j Hamiltonian

We use a rotationally invariant Hamiltonian with up to three-body interactions, acting between identical nucleons in a single-j orbital. Following the notation of Volya [13] we write the Hamiltonian as

$$\hat{H} = \hat{H}_1 + \hat{V}_2 + \hat{V}_3, \tag{1}$$

with

$$\begin{aligned}
\hat{H}_1 &= \epsilon_j \hat{n}_j = \epsilon_j \sum_{m=-j}^{+j} a^\dagger_{jm} a_{jm}, \\
\hat{V}_2 &= \sum_{J \text{ even}} V_J \sum_{M=-J}^{+J} \hat{T}^{(2)\dagger}_{JM} \hat{T}^{(2)}_{JM}, \\
\hat{V}_3 &= \sum_{J} \sum_{\alpha\alpha'} W_{J_{\alpha\alpha'}} \sum_{M=-J}^{+J} \hat{T}^{(3)\dagger}_{\alpha JM} \hat{T}^{(3)}_{\alpha' JM},
\end{aligned} \tag{2}$$

where $\hat{n}_j$ is the nucleon-number operator. The operator $a^\dagger_{jm}$ (a_{jm}) creates (annihilates) a nucleon in the orbital j with projection m; $\hat{T}^{(n)\dagger}_{\alpha JM}$ and $\hat{T}^{(n)}_{\alpha JM}$ are the generalization to operators that create and annihilate a normalized n-nucleon state with total angular momentum J and projection M. The notation α represents any additional label necessary to characterize fully the n-body state $|j^n \alpha JM\rangle$. The single-particle energy ϵ_j and the interactions

$$V_J \equiv \langle j^2 JM | \hat{V}_2 | j^2 JM \rangle, \quad W_{J_{\alpha\alpha'}} \equiv \langle j^3 \alpha JM | \hat{V}_3 | j^3 \alpha' JM \rangle, \tag{3}$$

completely determine the Hamiltonian (1) in a single-j orbital. In the two-body matrix elements no additional label α is needed and J must be even. In the three-body matrix elements additional labels are needed for certain values of J if $j \geq 9/2$ [15, 16].

Following Refs. [11, 12, 13] one can treat ϵ_j, V_J and $W_{J_{\alpha\alpha'}}$ as parameters to be fitted to the available binding energies of ground and excited states of semi-magic nuclei. Alternatively, one considers them as the matrix elements of an *effective* interaction, which arises due to truncation effects from a larger shell-model space to a single-j orbital. Expressions relevant to the latter approach are given in the next section.

3. Effective two- and three-body interactions

We consider a system of identical nucleons (neutrons or protons) in a valence shell containing several orbitals j, j_1, j_2,... with single-nucleon energies ϵ_j, ϵ_{j_1}, ϵ_{j_2},... The nucleons interact through a two-body force $\hat{V}_2$ and transitions of multipolarity λ between states are induced by one-body operators $\hat{T}^{(\lambda)}_1$. We assume that the orbital j is well below the others, $\epsilon_j \ll \epsilon_{j_1} \leq \epsilon_{j_2} \leq \cdots$. An equivalent problem arises for a system of orbitals j, j_1, j_2,... with single-nucleon energies $\epsilon_j \gg \epsilon_{j_1} \geq \epsilon_{j_2} \geq \cdots$, which can be reformulated in terms of holes. All formulas given below apply to this case as well after the substitution $\epsilon \to -\epsilon$.

The aim is to replace operators $\hat{O}$, defined for the entire shell-model space $\{j, j_1, j_2, \ldots\}$, by effective operators $\hat{O}_{\rm eff}$ that act in the single orbital j. This can be achieved most simply by considering, in the total Hamiltonian $\hat{H} = \hat{H}_1 + \hat{V}_2$, the two-body interaction $\hat{V}_2$ as a perturbation on the single-nucleon Hamiltonian $\hat{H}_1$, and by applying the perturbation method of Bloch and Horowitz [8]. For the definition of an effective interaction that contains up to and including three-body components, it is necessary to consider the perturbation due to $\hat{V}_2$ of one-, two- and three-nucleon states.

In the approximation outlined above, a state $|j\rangle$, with one nucleon in the orbital j and all others empty, cannot be perturbed by $\hat{V}_2$ since $\langle j|\hat{V}_2|j_k\rangle = 0$. The energy of this single-nucleon state is therefore

$$E^{(0)}(j) = \epsilon_j, \tag{4}$$

to all orders of perturbation theory and its perturbed wave function $|j)$ is the unperturbed wave function $|j\rangle$. Two-nucleon states have zeroth-order energies

$$E^{(0)}(j^2 J) = 2\epsilon_j, \tag{5}$$

and a first-order contribution of $\hat{V}_2$, which is its expectation value in the state $|j^2 J\rangle$,

$$E^{(1)}(j^2 J) = \langle j^2 J|\hat{V}_2|j^2 J\rangle \equiv V_J. \tag{6}$$

Similarly, three-nucleon states have zeroth-order energies

$$E^{(0)}(j^3 \alpha J) = 3\epsilon_j, \tag{7}$$

and a first-order contribution of $\hat{V}_2$, which is its expectation value in the state $|j^3 \alpha J\rangle$,

$$E^{(1)}(j^3 \alpha J) = \langle j^3 \alpha J|\hat{V}_2|j^3 \alpha J\rangle = 3\sum_R (c^R_{3\alpha J})^2 V_R, \tag{8}$$

where $c^{\alpha_{n-1} R}_{n\alpha_n J} \equiv [j^{n-1}(\alpha_{n-1} R) j J|\}j^n \alpha_n J]$ is an $n \to n-1$ coefficient of fractional parentage [15, 16]. The expressions for $E^{(n)}(j^2 J)$ and $E^{(n)}(j^3 \alpha J)$ in second ($n = 2$) and third ($n = 3$) order are given in Appendix A and Appendix B, respectively.

Up to order n of perturbation theory, an effective Hamiltonian with up to three-body interactions,

$$\hat{H}^{(n)}_{\rm eff} = \hat{H}^{(n)}_{\rm 1eff} + \hat{V}^{(n)}_{\rm 2eff} + \hat{V}^{(n)}_{\rm 3eff}, \tag{9}$$

can be constructed from

$$\begin{aligned}
&\langle j|\hat{H}^{(n)}_{\rm 1eff}|j\rangle = E^{(0)}(j) = \epsilon_j, \\
&\langle j^2 J|\hat{H}^{(n)}_{\rm eff}|j^2 J\rangle = \sum_{i=0}^{n} E^{(i)}(j^2 J), \\
&\langle j^3 \alpha J|\hat{H}^{(n)}_{\rm eff}|j^3 \alpha J\rangle = \sum_{i=0}^{n} E^{(i)}(j^3 \alpha J),
\end{aligned} \tag{10}$$

where the first, second, and third equation defines the 1-body, (1 + 2)-body, and (1 + 2 + 3)-body part of the effective Hamiltonian, respectively. The one-body part of

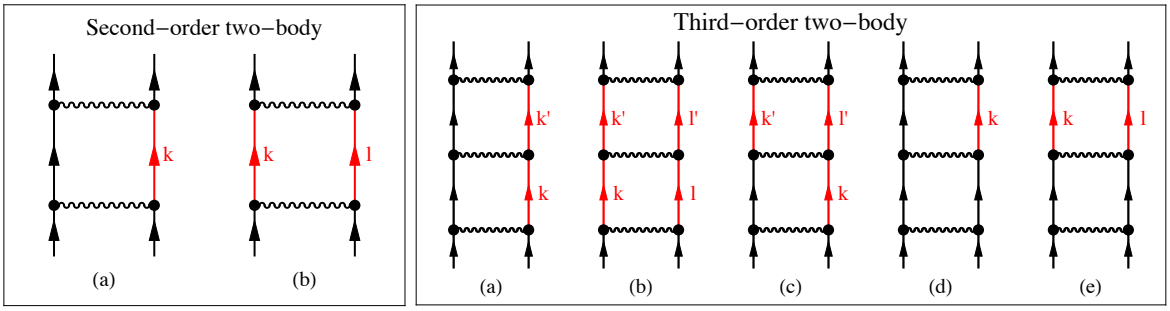

Figure 1. Second- and third-order contributions to the effective two-body interaction $\hat{V}_{2\text{eff}}$. The black unlabeled lines correspond to particles in the orbital j. Particle excitations into the orbitals j_k, j_l,... are indicated in red and labeled with the corresponding indices k, l,...

the effective Hamiltonian is $\hat{H}_{1\text{eff}} = \epsilon \hat{n}_j$ to all orders. The effective two-body interaction to order n is specified by the matrix elements

$$\langle j^2 J|\hat{V}^{(n)}_{2\text{eff}}|j^2 J\rangle = \sum_{i=1}^{n} E^{(i)}(j^2 J). \tag{11}$$

The effective three-body interaction to order n can be calculated from the third equation in Eq. (9). The contribution from the effective two-body interaction must be subtracted, leading to the following expression for the matrix elements of the effective three-body interaction:

$$\langle j^3 \alpha J|\hat{V}^{(n)}_{3\text{eff}}|j^3 \alpha J\rangle = \sum_{i=1}^{n} E^{(i)}(j^3 \alpha J) - 3\sum_{i=1}^{n}\sum_{R}(c^{R}_{3\alpha J})^2 E^{(i)}(j^2 R). \tag{12}$$

Care must be taken to compute both sums in this equation to the same order in perturbation theory. Because of Eqs. (6) and (8), this immediately shows that no three-body interaction occurs in first-order perturbation, $n = 1$. This is no longer the case for $n > 1$, as shown in Appendix A and Appendix B.

The different contributions to the effective Hamiltonian can be visualized with diagrams [8]. In view of the assumption $\epsilon_j \ll \epsilon_{j_1} \leq \epsilon_{j_2} \leq \cdots$, only particle excitations can occur and this considerably simplifies the enumeration of the diagrams. Still, a significant number of them survives, as shown in Figs. 1 and 2. In second order, two processes contribute to the effective two-body interaction $\hat{V}_{2\text{eff}}$ while only a single one is important for the effective three-body interaction $\hat{V}_{3\text{eff}}$ since the contribution of diagram (b) will be cancelled by that of the effective two-body interaction. This is a diagrammatic proof that, up to second order, $\hat{V}_{3\text{eff}}$ does not contain any contribution from the $|j_k j_l(L)jJ\rangle$ configurations [14]. In third order, the diagrams proliferate and, with the exception of diagram (c) of the effective three-body interaction $\hat{V}_{3\text{eff}}$, they all contribute.

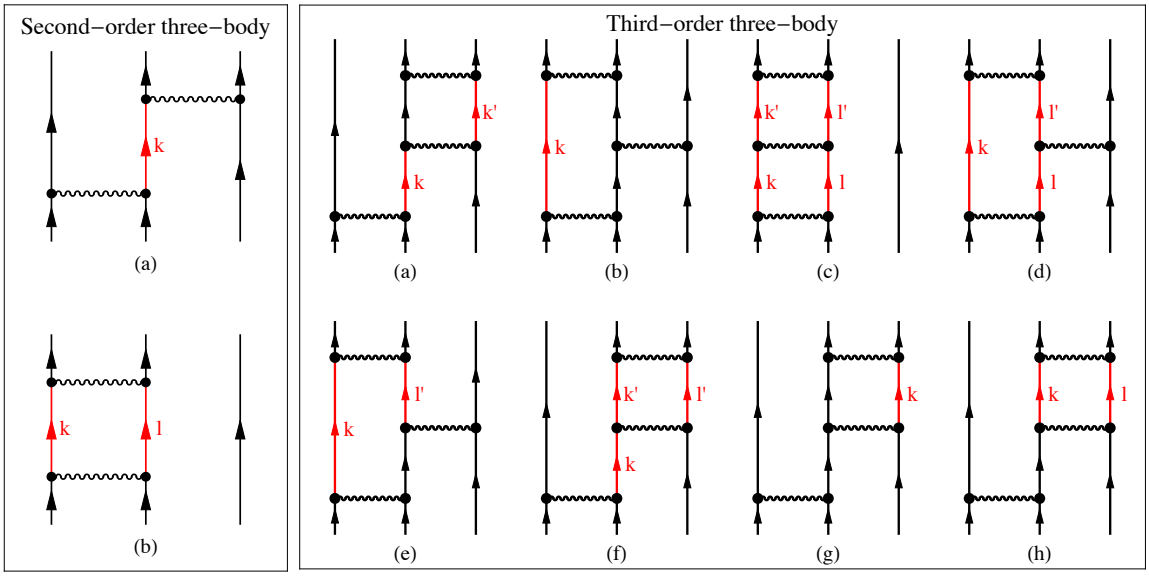

Figure 2. Same caption as Fig. 1 for the effective three-body interaction $\hat{V}_{3\text{eff}}$.

4. Effective one- and two-body transition operators

The same procedure can be followed to determine effective transition operators up two-body terms, starting from a one-body transition operator $\hat{T}_1$. The one-body part of the effective operator follows from the identity

$$\langle j\|\hat{T}^{(n)}_{1\text{eff}}\|j\rangle = (j\|\hat{T}_1\|j) = \langle j\|\hat{T}_1\|j\rangle, \tag{13}$$

which holds since the two-body interaction $\hat{V}_2$ does not perturb the single-nucleon state $|j\rangle$. We conclude that the one-body part of the effective operator coincides with the bare operator. This is not a general result from perturbation theory but specific to the zeroth-order approximation of one nucleon in the orbital j and completely empty orbitals j_1, j_2,...

Up to order n of perturbation theory, an effective operator with up to two-body terms,

$$\hat{T}^{(n)}_{\text{eff}} = \hat{T}^{(n)}_{1\text{eff}} + \hat{T}^{(n)}_{2\text{eff}}, \tag{14}$$

is obtained from the identity

$$\langle j^2 J_\text{f}\|\hat{T}^{(n)}_{\text{eff}}\|j^2 J_\text{i}\rangle = {}^{(n)}(j^2 J_\text{f}\|\hat{T}_1\|j^2 J_\text{i})^{(n)}, \tag{15}$$

where on the right-hand side wave functions to nth order in perturbation theory are used. The two-body part of the effective operator is therefore

$$\begin{aligned}\langle j^2 J_\text{f}\|\hat{T}^{(n)}_{2\text{eff}}\|j^2 J_\text{i}\rangle &= \langle j^2 J_\text{f}\|\hat{T}^{(n)}_{\text{eff}}\|j^2 J_\text{i}\rangle - \langle j^2 J_\text{f}\|\hat{T}^{(n)}_{1\text{eff}}\|j^2 J_\text{i}\rangle \\ &= {}^{(n)}(j^2 J_\text{f}\|\hat{T}_1\|j^2 J_\text{i})^{(n)} - \langle j^2 J_\text{f}\|\hat{T}_1\|j^2 J_\text{i}\rangle.\end{aligned} \tag{16}$$

Explicit expressions up to second order are given in Appendix C.

5. Recurrence relations

The matrix elements of a scalar k-body interaction $\hat{V}_k$ between two states belonging to the j^n configuration of n nucleons in the j orbital can be calculated from the recurrence relation [15, 16, 17, 18]

$$\langle j^n \alpha J|\hat{V}_k|j^n \alpha' J\rangle = \frac{n}{n-k} \sum_{\alpha_1 \alpha_1' J_1} c_{n\alpha J}^{\alpha_1 J_1} c_{n\alpha' J}^{\alpha_1' J_1} \langle j^{n-1} \alpha_1 J_1|\hat{V}_k|j^{n-1} \alpha_1' J_1\rangle. \quad (17)$$

This process is continued until matrix elements of $\hat{V}_k$ between states of the j^k configuration are reached. At that point the matrix elements (3) are inserted on the right-hand side of the recurrence relation, or their expressions in terms of the matrix elements of a larger shell-model space. Likewise, the matrix elements of a non-scalar k-body operator $\hat{T}_k(\lambda)$, where λ is its tensor character, can be obtained from

$$\langle j^n \alpha J\|\hat{T}_k(\lambda)\|j^n \alpha' J'\rangle = \frac{n}{n-k} \sum_{\alpha_1 J_1 \alpha_1' J_1'} (-)^{J_1+j+J'+\lambda} [J][J'] c_{n\alpha J}^{\alpha_1 J_1} c_{n\alpha' J'}^{\alpha_1' J_1'} \times \begin{Bmatrix} J_1 & J_1' & \lambda \\ J' & J & j \end{Bmatrix} \langle j^{n-1} \alpha_1 J_1\|\hat{T}_k(\lambda)\|j^{n-1} \alpha_1' J_1'\rangle, \quad (18)$$

with $[x] \equiv \sqrt{2x+1}$, and this process can be applied up to the matrix elements $\langle j^k \alpha_1 J_1\|\hat{T}_k(\lambda)\|j^k \alpha_1' J_1'\rangle$.

6. Applications

6.1. Empirical fits

We first ask the question whether there exists any evidence for the presence of three-body forces in the context of a single-orbital calculation. This question can be answered by considering either the Hamiltonian $\hat{H}_1+\hat{V}_2$ or the Hamiltonian $\hat{H}_1+\hat{V}_2+\hat{V}_3$, adjusting the interaction matrix elements (3) to the available data, and comparing the relative merits of both calculations. Theoretical spectra are obtained after minimizing, with respect to V_J and $W_{J_{\alpha\alpha'}}$, the quantity

$$\chi = \sqrt{\frac{1}{N-N_\mathrm{p}} \sum_k \frac{\left[BE_\mathrm{exp}(k) - BE_\mathrm{th}(k)\right]^2}{\sigma_\mathrm{exp}^2(k) + \sigma^2}}, \quad (19)$$

where 'BE' stands for binding energy, either experimental or calculated, and where the sum runs over all data points, which are N in number, and N_p is the number of parameters. Furthermore, $\sigma_\mathrm{exp}(k)$ is the experimental uncertainty on the k^th energy. This uncertainty, predominantly due to that on the binding energies, is in most cases of the order of a few keV and therefore well below the root-mean-square deviation defined as

$$\sigma = \sqrt{\frac{1}{N} \sum_k \left[BE_\mathrm{exp}(k) - BE_\mathrm{th}(k)\right]^2}. \quad (20)$$

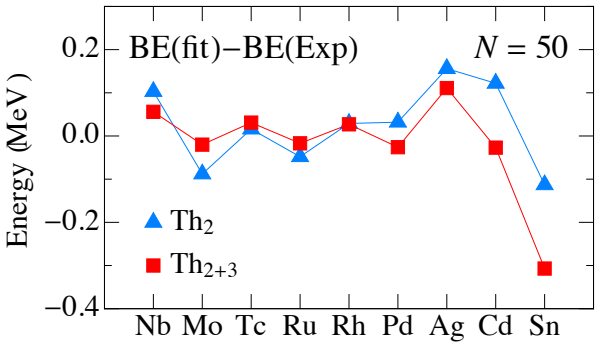

Figure 3. The difference between calculated and experimental ground-state binding energies of $N = 50$ isotones. The theoretical values are calculated with two-body interactions (Th_2) or with two- and three-body interactions (Th_{2+3}), with the χ-minimum parameters of Table 1.

We include therefore in Eq. (19) the deviation σ, which can be viewed as an additional 'theoretical uncertainty' on the energy.

6.1.1. The $N = 50$ isotones A good test case is provided by the $N = 50$ isotones with Z ranging from 40 (zirconium) to 50 (tin) when the protons are dominantly in the $0g_{9/2}$ orbital. A total of 45 energies are known experimentally. The ground-state binding energies are taken from Ref. [19] and the excitation energies from NNDC [20], with some additional information from Refs. [21, 22]. Two fits are carried out, one with two-body interactions (Th_2) and another one with two-plus-three-body interactions (Th_{2+3}). In the former case there are five matrix elements V_J with $J = 0$, 2, 4, 6 and 8. In the Th_{2+3} calculation this set is augmented with the three-body matrix elements $W_{J_{\alpha\alpha'}}$ with $J = 3/2$, 5/2, 7/2, 9/2, 11/2, 13/2, 15/2, 17/2 and 21/2. States are unique for $J \neq 9/2$ and no additional label α is needed. For $J = 9/2$ there are two independent states in the $|j^3 \alpha J\rangle$ configuration, and therefore two diagonal matrix elements and an off-diagonal one. In following we only consider the diagonal matrix elements, $W_{J_{\alpha\alpha}}$, which we denote as W_{J_α}, and neglect the off-diagonal matrix element $W_{J_{\alpha\alpha'}}$. As absolute energies are calculated, the single-particle energy $\epsilon_{9/2}$ must be considered as an additional parameter in both fits.

The results concerning the binding energies are shown in Fig. 3 and energy spectra are plotted in Fig. 4, which contains most of the levels included in the fits. In each case we display the results of the two fits, Th_2 and Th_{2+3}. One observes from Fig. 3 that the addition of a three-body interaction does not notably improve the quality of the fit. Comments about the energy spectra will be made at the end of Subsect. 6.1.2.

The interaction matrix elements resulting from the two fits are shown in the two columns labeled 'χ minimum' of Table 1. Although the number of parameters increases from six to sixteen between the two fits Th_2 and Th_{2+3}, the value of χ at the minimum is smaller by about 30 % in the latter calculation. This indicates that the three-body interaction meaningfully improves the results. The value of σ is about the same in the

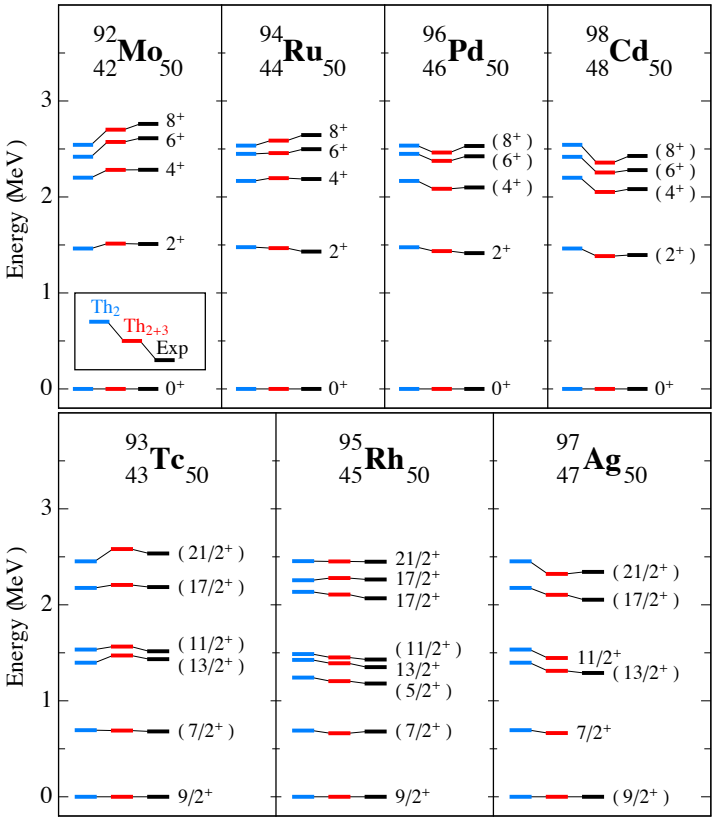

Figure 4. Excitation spectra of the even-mass and odd-mass $N = 50$ isotones. Experimental energies (Exp) are compared to those calculated with two-body interactions (Th_2) or with two- and three-body interactions (Th_{2+3}), with the χ-minimum parameters of Table 1.

two calculations because of a single large deviation in Th_{2+3} for ^{100}Sn (see Fig. 3). As the uncertainty on the binding energy of this nucleus is large (300 keV) [19] this has not much impact on the value of χ but it does increase σ significantly.

Table 1 also lists the uncertainties on the different matrix elements. They are obtained from the diagonalization of the covariance matrix, leading to uncorrelated parameters and their associated uncertainties, from which those on the initial parameters can be computed. The uncertainties thus obtained must be considered as an extreme lower limit on the actual uncertainties on the fitted matrix elements because they do not include effects from the variation of the input data. The latter effects are illustrated in the fits labeled 'σ minimum' and 'χ' minimum' in Table 1. In the former fit experimental uncertainties are ignored and the minimized quantity is the root-mean-square deviation σ in Eq. (20). As the uncertainties on the binding energies of ^{97}Ag, ^{98}Cd and ^{100}Sn are rather large [19], the 'χ-minimum' fit gives therefore less weight to the data concerning the proton-rich isotopes. It is seen that, while the Th_2 results are stable against this change, the Th_{2+3} results are not, and in particular the three-body matrix elements fluctuate wildly. Likewise, in the fit labeled 'χ' minimum' in Table 1 a *single* level is added to the input data, namely a second 6^+ level ^{94}Ru, for which there exists some

Table 1. Two- and three-body matrix elements (in keV) and the χ and σ deviations of Eqs. (19) and (20) for the various fits to the $N = 50$ isotones described in the text.

	χ minimum		σ minimum		χ' minimum	
	Th_2	Th_{2+3}	Th_2	Th_{2+3}	Th_2	Th_{2+3}
$\epsilon_{9/2}$	−5251	−5204 (1)	−5249	−5227	−5255	−5209
V_0	−2011	−2174 (3)	−2002	−2157	−2000	−2158
V_2	−548	−659 (3)	−550	−637	−564	−682
V_4	189	108 (2)	188	149	197	124
V_6	407	399 (2)	405	432	414	416
V_8	532	528 (2)	533	537	531	523
$W_{3/2}$	—	256 (63)	—	397	—	293
$W_{5/2}$	—	−54 (16)	—	−46	—	−94
$W_{7/2}$	—	53 (6)	—	42	—	43
$W_{9/2_1}$	—	47 (1)	—	37	—	43
$W_{9/2_2}$	—	−112 (57)	—	−256	—	−125
$W_{11/2}$	—	35 (8)	—	33	—	58
$W_{13/2}$	—	46 (2)	—	32	—	70
$W_{15/2}$	—	55 (18)	—	92	—	55
$W_{17/2}$	—	−43 (5)	—	−62	—	−81
$W_{21/2}$	—	−12 (4)	—	−17	—	−1
χ^a	0.946	0.671	0.954	1.039	0.987	0.885
σ	63	62	63	46	78	70

[a]Dimensionless.

evidence [21]. Again one observes stability of the Th_2 and fluctuations of the Th_{2+3} matrix elements.

6.1.2. The lead isotopes A similar application is possible for the Pb isotopes, where the protons form a closed shell and the neutrons are predominantly in the $1g_{9/2}$ orbital. Less data are available as compared to the case of the $N = 50$ isotones, and in particular measured quantities are lacking for the most neutron-rich Pb isotopes. The ground-state binding energies are taken from Ref. [19] and the excitation energies from Refs. [20, 23]. To extend the fit over the entire range of isotopes from ^{208}Pb to ^{218}Pb, we use extrapolated atomic masses for ^{216,217,218}Pb together with their associated (rather large) estimated uncertainties [19]. The angular momentum of the single-particle orbital is $j = 9/2$ as in the case of the $N = 50$ isotones and therefore the same set of two- and three-body matrix elements is adjusted to the data.

The results concerning the binding energies are shown in Fig. 5 and energy spectra are plotted in Fig. 6, which contains most of the levels included in the fits. In each case we display the results of the two fits, Th_2 and Th_{2+3}. Again one observes from Fig. 5 that the addition of a three-body interaction does not notably improve the quality of

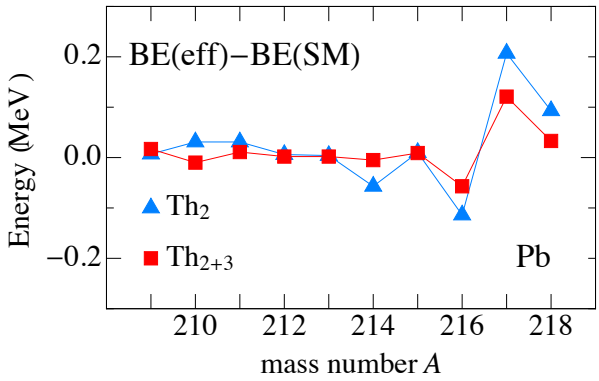

Figure 5. The difference between calculated and experimental ground-state binding energies of Pb isotopes. The theoretical values are calculated with two-body interactions (Th_2) or with two- and three-body interactions (Th_{2+3}), with the χ-minimum parameters of Table 2.

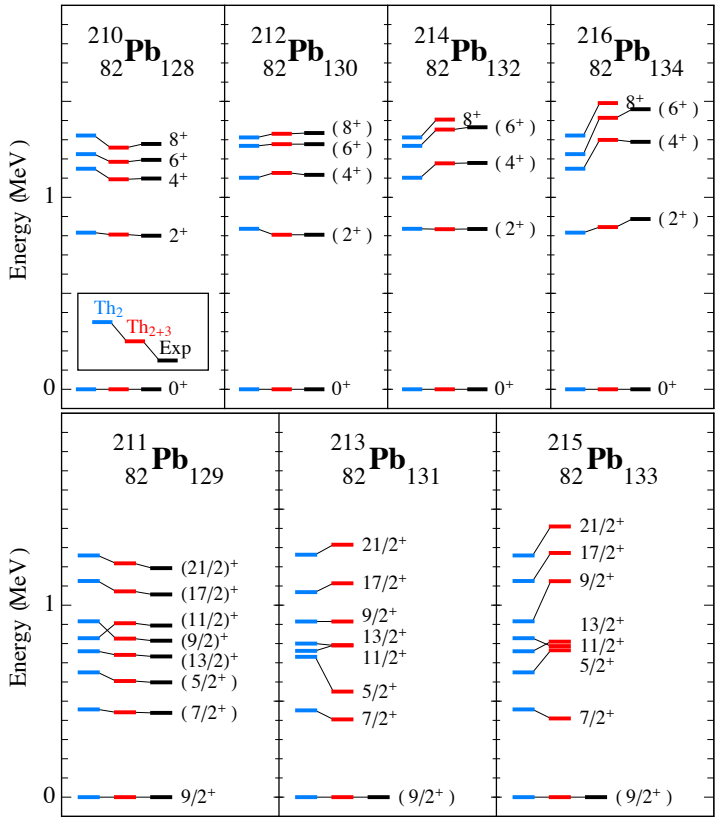

Figure 6. Excitation spectra of the the even-mass and odd-mass Pb isotones. Experimental energies (Exp) are compared to those calculated with two-body interactions (Th_2) or with two- and three-body interactions (Th_{2+3}), with the χ-minimum parameters of Table 2.

Table 2. Two- and three-body matrix elements (in keV) and the χ and σ deviations of Eqs. (19) and (20) for the various fits to the Pb isotopes described in the text.

	χ minimum		σ minimum		χ' minimum	
	Th_2	Th_{2+3}	Th_2	Th_{2+3}	Th_2	Th_{2+3}
$\epsilon_{9/2}$	−3944	−3954 (1)	−3944	−3961	−3952	−3964
$V_0^{(2)}$	−1266	−1203 (2)	−1296	−1176	−1249	−1177
$V_2^{(2)}$	−450	−398 (1)	−463	−381	−445	−407
$V_4^{(2)}$	−117	−109 (1)	−123	−81	−150	−119
$V_6^{(2)}$	−41	−19 (1)	−29	−5	−19	−3
$V_8^{(2)}$	56	55 (1)	62	44	61	66
$W_{3/2}$	—	0 (14)	—	−46	—	219
$W_{5/2}$	—	−75 (2)	—	−104	—	−42
$W_{7/2}$	—	−47 (1)	—	−46	—	5
$W_{9/2_1}$	—	−29 (1)	—	−42	—	−34
$W_{9/2_2}$	—	−83 (4)	—	−117	—	−50
$W_{11/2}$	—	88 (2)	—	60	—	−99
$W_{13/2}$	—	−31 (1)	—	−31	—	5
$W_{15/2}$	—	73 (1)	—	64	—	42
$W_{17/2}$	—	−17 (2)	—	−5	—	5
$W_{21/2}$	—	−2 (1)	—	36	—	−4
χ^a	0.629	0.371	0.769	0.897	0.656	0.578
σ	60	29	53	21	59	35

[a]Dimensionless.

the fit.

In addition, Table 2 lists the interaction matrix elements obtained in three different fits. Two of them, labeled 'χ minimum' and 'σ minimum', adjust the parameters by minimizing χ and σ of Eqs. (19) and (20), respectively. In the isotope ^{211}Pb two $11/2^+$ levels occur at 643 and 894 keV, respectively, and it is not *a priori* clear which level belongs to the $(1g_{9/2})^3$ configuration and which is the $0i_{11/2}$ single-particle state. In the χ-minimum fit we assume $11/2_2^+$ is the single-particle state while in the χ'-minimum fit we identify it with $11/2_1^+$. The conclusions to be drawn from these results are consistent with those obtained from the analysis of the $N = 50$ isotones: stability of the Th_2 matrix elements and large fluctuations of those in the Th_{2+3} fit.

It should be stressed that, in spite of the difficulties in determining the strengths of the components of the three-body interaction, there is unmistakable evidence for its presence. The spectra of even-even nuclei shown in Figs. 4 and 6 most clearly illustrate this evidence. Both in the $N = 50$ isotones and in the Pb isotopes one observes a clear variation of the experimental spectra with mass number A: In the former case the spectrum compresses with A while in the latter case it expands. This trend cannot be reproduced with a two-body interaction alone since, as a result of the particle-

hole symmetry of the two-body interaction, the particle-hole conjugated spectra in the Th_2 calculation are the same. Therefore, the spectra of the pairs ^{92}Mo-^{98}Cd, ^{94}Ru-^{96}Pd and the pairs ^{210}Pb-^{216}Pb, ^{212}Pb-^{214}Pb are identical in Th_2. It is obvious that experimentally they are not and that the observed trend can be reproduced with a three-body interaction. However, for the $N = 50$ isotones and for the Pb isotopes at least, the available spectroscopic data are insufficient to determine reliably the separate components of the three-body interaction.

6.2. Effective operators in a single-j orbital

From the previous subsection we conclude that the three-body component of the nuclear interaction is difficult to obtain reliably from an empirical fit. Also, if a three-body interaction is considered in the Hamiltonian, a consistent approach requires the consideration of two-body terms in transition operators—even less obtainable from data. Therefore some microscopic input is needed.

We take as starting point a realistic two-body interaction in a large shell-model space together with appropriate single-particle energies. For the $N = 50$ isotones we consider protons in the orbitals $0f_{5/2}$, $1p_{3/2}$, $1p_{1/2}$ and $0g_{9/2}$, interacting via the $T = 1$ force from Lisetskiy *et al.* [24]. For the Pb isotopes we consider neutrons in the orbitals $0i_{11/2}$, $1g_{9/2}$, $1g_{7/2}$, $2d_{5/2}$, $2d_{3/2}$, $3s_{1/2}$ and $0j_{15/2}$, together with the Kuo-Herling interaction [25, 26].

Before anything else, it is necessary to check whether the single-j orbital, $0g_{9/2}$ for the protons in the $N = 50$ isotones and $1g_{9/2}$ for the neutrons in the Pb isotopes, is sufficiently isolated from the other orbitals in the respective shell-model spaces for the perturbation approximation to be valid. This can be achieved by comparing the results of a full shell-model calculation with those obtained with an effective interaction in a single-j orbital. This comparison is made in Table 3 for nuclei with two and three valence proton holes in $0g_{9/2}$, and two and three valence neutron particles in $1g_{9/2}$. The second and third columns list the binding energies obtained in a single-j orbital with an effective two-body interaction calculated up to first and second order, respectively. The fourth column adds to this the contribution of the effective three-body interaction, calculated up to second order. The fifth and sixth columns give the result of the calculation up to third order without and with an effective three-body interaction, respectively. The seventh column, labeled 'SM', lists the binding energies obtained in the full shell-model space. In all cases binding energies are given relative to the appropriate core, either ^{100}Sn or ^{208}Pb.

A few comments about Table 3 are in order. Convergence towards the shell-model results is obtained to within a few tens of keV and perturbation theory up to second order usually suffices. The third-order correction to the effective two-body interaction is significant only for the pairing matrix element, which shows up in the 0^+ binding energy in ^{98}Cd and ^{210}Pb and that of the $9/2^+_1$ state in ^{97}Ag and ^{211}Pb. The contribution of the three-body interaction is seen to be small. It is obviously the case that the

Table 3. Binding energies of levels in ^{98}Cd and ^{97}Ag, relative to ^{100}Sn, and of levels in ^{210}Pb and ^{211}Pb, relative to ^{208}Pb, calculated with various effective interactions in a single-j orbital and compared with the full shell-model results (SM).

		Energy (MeV)					
Nucleus	J^π	$\hat{V}^{(1)}_{\rm 2eff}$	$\hat{V}^{(2)}_{\rm 2eff}$	$\hat{V}^{(2)}_{\rm 23eff}$	$\hat{V}^{(3)}_{\rm 2eff}$	$\hat{V}^{(3)}_{\rm 23eff}$	SM
^{98}Cd	0^+	−4.532	−3.615	−3.615	−3.776	−3.776	−3.786
	2^+	−5.259	−5.145	−5.145	−5.133	−5.133	−5.132
	4^+	−5.897	−5.865	−5.865	−5.864	−5.864	−5.864
	6^+	−6.120	−6.120	−6.120	−6.120	−6.120	−6.120
	8^+	−6.307	−6.307	−6.307	−6.307	−6.307	−6.307
^{97}Ag	$3/2^+$	−9.355	−9.286	−9.286	−9.283	−9.270	−9.266
	$5/2^+$	−8.993	−8.879	−8.879	−8.869	−8.857	−8.842
	$7/2^+$	−8.580	−8.386	−8.386	−8.367	−8.354	−8.357
	$9/2^+_1$	−8.414	−7.639	−7.639	−7.764	−7.694	−7.734
	$9/2^+_2$	−9.502	−9.449	−9.449	−9.446	−9.445	−9.444
	$11/2^+$	−9.313	−9.216	−9.216	−9.209	−9.211	−9.210
	$13/2^+$	−9.229	−9.119	−9.119	−9.109	−9.109	−9.104
	$15/2^+$	−9.883	−9.870	−9.870	−9.870	−9.870	−9.870
	$17/2^+$	−9.949	−9.921	−9.921	−9.920	−9.918	−9.918
	$21/2^+$	−10.274	−10.274	−10.274	−10.274	−10.274	−10.274
^{210}Pb	0^+	8.402	8.804	8.804	9.067	9.067	9.091
	2^+	8.156	8.228	8.228	8.248	8.248	8.254
	4^+	7.953	7.982	7.982	7.989	7.989	7.992
	6^+	7.877	7.895	7.895	7.899	7.899	7.900
	8^+	7.837	7.852	7.852	7.856	7.856	7.856
^{211}Pb	$3/2^+$	11.986	12.064	12.072	12.083	12.098	12.109
	$5/2^+$	12.097	12.202	12.211	12.230	12.243	12.253
	$7/2^+$	12.252	12.392	12.402	12.430	12.435	12.436
	$9/2^+_1$	12.310	12.687	12.688	12.911	12.892	12.936
	$9/2^+_2$	11.939	12.012	12.001	12.029	12.011	12.012
	$11/2^+$	12.016	12.108	12.092	12.131	12.106	12.106
	$13/2^+$	12.043	12.145	12.135	12.171	12.156	12.161
	$15/2^+$	11.822	11.879	11.871	11.891	11.878	11.878
	$17/2^+$	11.823	11.882	11.879	11.895	11.890	11.892
	$21/2^+$	11.728	11.776	11.775	11.786	11.783	11.784

effective three-body interaction cannot contribute to the binding energy of ^{98}Cd and ^{210}Pb. In second order it also does not contribute to that of the three-hole nucleus ^{97}Ag. This can be understood from Eq. (B.4) [or, alternatively, the second-order diagram (a) in Fig. 2] which contains the matrix elements $V_k^R = \langle j^2 R|\hat{V}_2|jj_kR\rangle$, with $j = 0g_{9/2}$ and $j_k = 0f_{5/2}, 1p_{3/2}, 1p_{1/2}$, and which therefore vanish because of parity conservation. However, in third order the effective three-body interaction in ^{97}Ag does not vanish because the diagrams (d) and (h) in Fig. 2 are parity conserving.

If we compare the results of the calculation with a two-plus-three-body effective interaction up to third order (penultimate column '$\hat{V}^{(3)}_{23\mathrm{eff}}$' in Table 3) with those of the shell model, we can conclude that the numbers agree closely, except for the 0^+ state in the two-nucleon and the $9/2^+_1$ state in the three-nucleon nuclei. For example, the 0^+ level in ^{210}Pb is underbound by 24 keV and the $9/2^+_1$ level in ^{211}Pb by 44 keV. These discrepancies correspond to a two-body pairing matrix element

$$V_0 = \langle j^2, \upsilon = 0, J = 0|\hat{V}_2|j^2, \upsilon = 0, J = 0\rangle, \tag{21}$$

that is 24 keV less attractive than it should be and a 'three-body pairing matrix element'

$$W_{9/2_1} = \langle j^3, \upsilon = 1, J = j|\hat{V}_3|j^3, \upsilon = 1, J = j\rangle, \tag{22}$$

that is 24.2 keV less attractive than it should be. These discrepancies might seem insignificant for low valence nucleon number n but they lead to important deviations for higher n. An estimate of the resulting corrections can be obtained by noting that a Hamiltonian with a two-body *and* a three-body pairing interaction in the $j = 9/2$ orbital has the ground-state eigenvalues [29]

$$(n-\upsilon)(12-n-\upsilon)\left[\frac{1}{20}V_0 + \frac{1}{16}(n-2)W_{9/2_1}\right], \tag{23}$$

where the seniority υ is 0 (1) for even (odd) n. If the strengths of the pairing interactions are off by tens of keV, we conclude from Eq. (23) that it leads to deviations of several hundreds of keV for $n = 10$.

Corresponding results for $E2$ transitions are shown in Table 4 for the nuclei ^{98}Cd and ^{210}Pb. The structure of the initial and final two-particle states is fixed and therefore the $B(E2)$ values do not depend on the effective interaction. The third column lists $B(E2)$ values obtained with the standard one-body $E2$ operator $\sum_i r_i^2 Y_{2\mu}(\theta_i, \phi_i)$ in a single-j orbital. The fourth and fifth columns add to this the contribution from the effective two-body operator, calculated up to first and second order, respectively. Perturbation theory converges reasonably close to the full shell-model results, except for the $2^+ \to 0^+$ transitions. This might be due to the difficulty in capturing the structure of a correlated pairing state in a perturbation approach. Furthermore, in ^{98}Cd the two-body part of the $E2$ operator vanishes in first-order perturbation theory, which can be understood from Eq. (C.6) and the zero matrix elements $V_k^J = \langle j^2 J|\hat{V}_2|jj_kJ\rangle$. Corrections to the one-body operator then only arise because of some second-order terms in the expression (C.8) and they are seen to be small or unreliable in the case of the $2^+ \to 0^+$ transition.

We conclude that the model space employed here for the $N = 50$ isotones, consisting of the $0f_{5/2}$, $1p_{3/2}$, $1p_{1/2}$ and $0g_{9/2}$ orbitals, leads to an effective three-body interaction

Table 4. $B(E2; J_{\rm i}^{\pi} \to J_{\rm f}^{\pi})$ values (in units e^2b^4, with b the oscillator length) for transitions in ^{98}Cd and ^{210}Pb, calculated with various effective $E2$ operators in a single-j orbital and compared with the full shell-model results (SM).

		$B(E2; J_{\rm i}^{\pi} \to J_{\rm f}^{\pi})$			
Nucleus	$J_{\rm i}^{\pi} \to J_{\rm f}^{\pi}$	$\hat{T}_1$	$\hat{T}^{(1)}_{12\rm eff}$	$\hat{T}^{(2)}_{12\rm eff}$	SM
^{98}Cd	$2^+ \to 0^+$	2.334	2.334	1.661	2.243
	$4^+ \to 2^+$	2.682	2.682	2.614	2.649
	$6^+ \to 4^+$	1.855	1.855	1.848	1.847
	$8^+ \to 6^+$	0.743	0.743	0.743	0.743
^{210}Pb	$2^+ \to 0^+$	4.341	5.050	4.918	4.462
	$4^+ \to 2^+$	4.987	5.671	5.820	5.933
	$6^+ \to 4^+$	3.449	3.947	4.046	4.152
	$8^+ \to 6^+$	1.381	1.633	1.704	1.754

and an effective two-body $E2$ operator that vanish in leading order. A recent study [27] of ^{94}Ru and ^{96}Pd arrives at a related conclusion, namely that the spectroscopy of the $N = 50$ isotones is best reproduced in a large-scale shell-model calculation with a single-particle space that includes the orbitals $0g$, $1d$ and $2s$ of the $N = 4$ major oscillator shell. On the other hand, the model space employed for the Pb isotopes leads to effective operators that do not vanish in leading order and, therefore, we concentrate from now on on the latter. We also conclude from Table 3 that it is necessary to include diagrams up to at least third order, which is what is done in the following.

The results concerning the binding energies of the Pb isotopes are displayed in Fig. 7 and those concerning their excitation spectra in Fig. 8. Calculations with four different effective interactions are shown: (a) an effective two-body interaction $\hat{V}^{(3)}_{2\rm eff}$ calculated up to third order; (b) an 'exact' effective two-body interaction $\hat{V}^{(\infty)}_{2\rm eff}$; (c) an effective two-plus-three-body interaction $\hat{V}^{(3)}_{23\rm eff}$ calculated up to third order; (d) an 'exact' effective two-plus-three-body interaction $\hat{V}^{(\infty)}_{23\rm eff}$. The approximations (a) and (c) are obtained with use of the perturbation expressions given in Sect. 3 and in Appendix A and Appendix B. The exact effective two-body interaction is obtained by reproducing the shell-model results for two nucleons and the exact effective two-plus-three-body interaction by reproducing the shell-model results for two and three nucleons.

A word of clarification is needed concerning the use of these so-called exact effective interactions. We in fact can show that, for two nucleons, the use of such an exact effective interaction is entirely equivalent to the method of Okubo, Lee and Suzuki (OLS) [30, 31], which determines effective operators in a restricted space. To see this point, we introduce the notions of a restricted Hilbert space $\hat{P}\mathbb{H}$ (i.e., here the model space constructed from the single-j orbital) and of an excluded Hilbert space $\hat{Q}\mathbb{H}$, such that $(\hat{P}+\hat{Q})\mathbb{H} = \mathbb{H}$ is the total Hilbert space (i.e., here the full shell-model space). Any eigenstate $|\phi\rangle$ of the Hamiltonian $\hat{H}$ in the full shell-model space has a component $\hat{P}|\phi\rangle$ in the restricted space and a component $\hat{Q}|\phi\rangle$ outside the restricted space. In the OLS

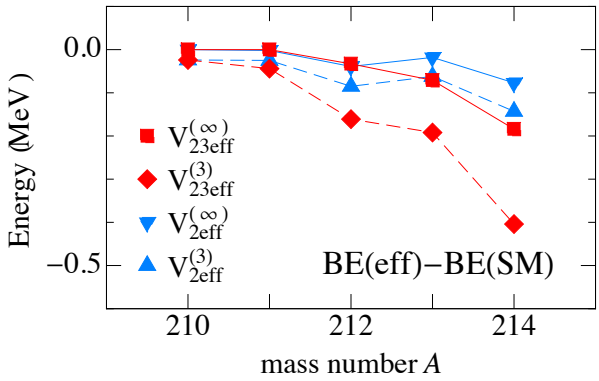

Figure 7. The difference between ground-state binding energies of the Pb isotopes, calculated with various effective interactions, and those obtained in the full shell-model space. The different effective interactions are: (a) effective two-body interaction calculated up to third order (blue triangles, dashed line); (b) exact effective two-body interaction (blue triangles, full line); (c) effective two-plus-three-body interaction calculated up to third order (red squares, dashed line); (d) exact effective two-plus-three-body interaction (red squares, full line).

method an operator $\hat{\eta}$ is constructed that maps states in $\hat{Q}\mathbb{H}$ onto states in $\hat{P}\mathbb{H}$ such that $\eta\hat{P}|\phi_i\rangle = \hat{Q}|\phi_i\rangle$ for a particular subset of eigenstates $|\phi_i\rangle$. It can be shown that the eigenvalues of the transformed (non-Hermitian) Hamiltonian $(\hat{I}-\hat{\eta})\hat{H}(\hat{I}+\hat{\eta})$ (where $\hat{I}$ is the identity operator) in the restricted space $\hat{P}\mathbb{H}$ coincide *exactly* with a subset of the eigenvalues of $\hat{H}$ in $\mathbb{H}$. The effective Hamiltonian in the OLS approach is finally obtained after a further transformation to make $(\hat{I}-\hat{\eta})\hat{H}(\hat{I}+\hat{\eta})$ Hermitian.

For two nucleons in a single-j orbital there exists only one state of a given angular momentum and the OLS method therefore ensures that the expectation value of the effective Hamiltonian in this state coincides with the eigenvalue corresponding to the eigenstate of the full Hamiltonian that has the dominant single-j component. This shows that the effective two-body interaction $\hat{V}_{2\mathrm{eff}}^{(\infty)}$ used here is the same as that obtained with the OLS method.

The same argument can be made for three nucleons in a single-j orbital provided only one state exists with angular momentum J. For the orbitals considered here with $j = 9/2$ this is always the case except when the three nucleons couple to $J = 9/2$, which has two independent states. For $J = 9/2$ the OLS method yields a 2×2 matrix whose eigenvalues coincide exactly with two of the eigenvalues of the Hamiltonian in the full space. In general, this 2×2 matrix will have a non-zero off-diagonal element while we have assumed in the construction of the $\hat{V}_{3\mathrm{eff}}^{(\infty)}$ interaction that this matrix element is zero. We therefore conclude that the exact effective interaction used here is equivalent to the one obtained with the OLS method, provided that the off-diagonal matrix element for $J = 9/2$ can be neglected, as is done throughout this paper. Under this assumption one can dispense with the OLS formalism, and simply fix the effective matrix elements such that they reproduce the shell-model results of the two- and three-nucleon systems.

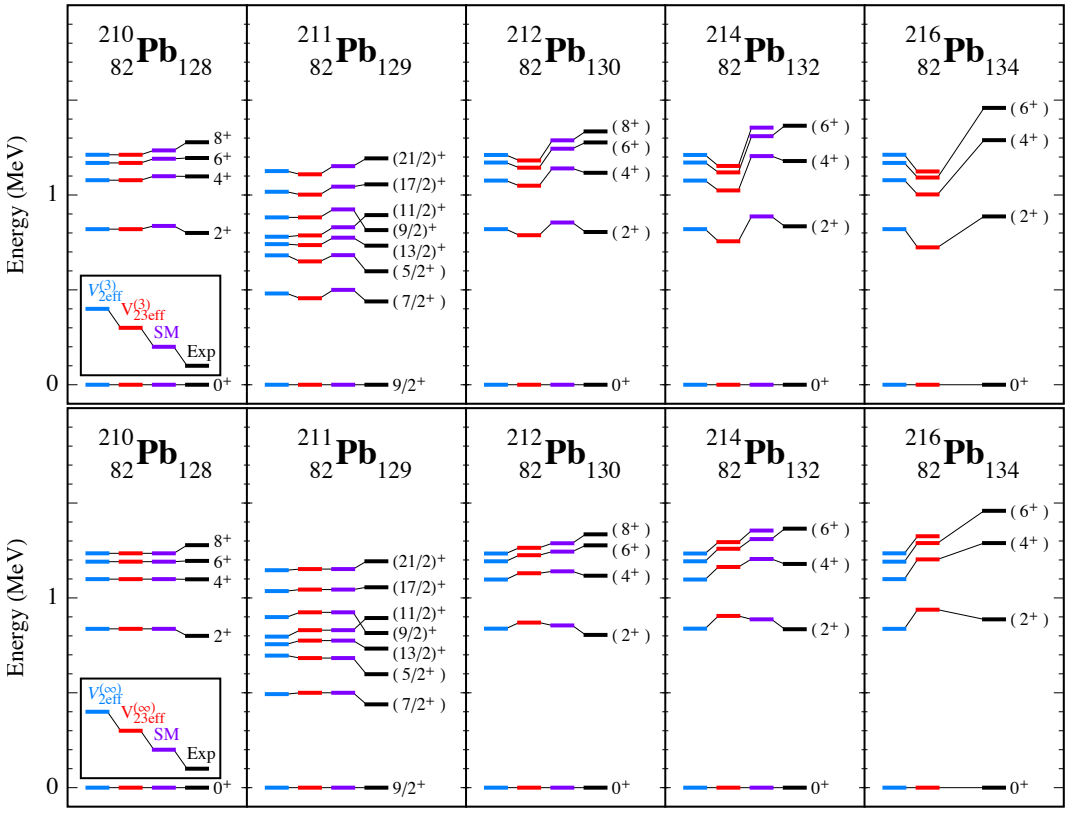

Figure 8. Experimental energies (Exp) of levels in the Pb isotopes compared with energies calculated with various effective interactions in a single-j orbital and with those calculated in the full shell model (SM). In the upper panel the effective interaction is calculated up to third order in perturbation theory, and is either of two-body (blue) or two-plus-three-body (red) character. In the lower panel the exact effective interaction is taken (see text), either of two-body (blue) or two-plus-three-body (red) character.

We first discuss the binding energies of the ground states since these are often used to unveil the presence of three-body forces [32]. To visualize the results, we plot in Fig. 7 the difference between binding energies, calculated with the various effective interactions, and those obtained in the full shell-model space. The conclusion is clear: Adding a three-body component to the effective interaction does not improve the description of the binding energies. A possible (but unlikely) explanation is that the off-diagonal matrix element $\langle j^3, \upsilon = 1, 9/2|\hat{V}_3|j^3, \upsilon = 3, 9/2\rangle$, here neglected, is crucial to the description of binding energies. A more likely explanation is that the pairing correlations are such that an effective interaction requires a four-body component. Another conclusion that can be drawn from Fig. 7 is that a perturbation calculation that stops at third order is not sufficient, certainly not for the effective three-body interaction.

While it is hard to tell whether there exists any empirical evidence for higher-body interactions based on binding energies, their presence is evident from excitation energies, as shown in Fig. 8. With increasing mass number A the observed spectra (labeled 'Exp' in the figure) of the even-even Pb isotopes expand. For example, the 2^+ energy increases

Table 5. $B(E2; J_\mathrm{i}^\pi \to J_\mathrm{f}^\pi)$ values for transitions in the even Pb isotopes, calculated with various $E2$ operators in a single-j orbital and compared with the measured values where available.

		$B(E2; J_\mathrm{i}^\pi \to J_\mathrm{f}^\pi)$ $(e^2\mathrm{fm}^4)$					
Nucleus	$J_\mathrm{i}^\pi \to J_\mathrm{f}^\pi$	$\hat{T}_1$	$\hat{T}^{(1)}_{12\mathrm{eff}}$	$\hat{T}^{(2)}_{12\mathrm{eff}}$	$+\hat{V}^{(3)}_{23\mathrm{eff}}$	SM	Exp
$A = 210$	$2^+ \to 0^+$	94	109	106	106	104	105 (30)
	$4^+ \to 2^+$	108	122	126	126	138	360 (68)
	$6^+ \to 4^+$	74	85	88	88	97	158 (60)
	$8^+ \to 6^+$	30	35	37	37	41	53 (23)
$A = 212$	$2^+ \to 0^+$	140	176	174	174	210	—
	$4^+ \to 2^+$	12	16	18	32	68	—
	$6^+ \to 4^+$	8	9	11	9	28	—
	$8^+ \to 6^+$	3	3	4	2	8	∼2
$A = 214$	$2^+ \to 0^+$	140	189	189	189	304	—
	$4^+ \to 2^+$	12	16	13	3	9	—
	$6^+ \to 4^+$	8	12	10	15	0.1	—
	$8^+ \to 6^+$	3	5	4	6	0.3	∼2
$A = 216$	$2^+ \to 0^+$	94	135	137	137	—	—
	$4^+ \to 2^+$	108	158	153	153	—	—
	$6^+ \to 4^+$	74	109	105	105	—	—
	$8^+ \to 6^+$	30	42	40	40	—	∼25

from 0.800 MeV in ^{210}Pb to 0.887 MeV in ^{216}Pb. This trend is correctly reproduced by the shell model in the full space (labeled 'SM' in the figure). All two-body interactions satisfy particle-hole symmetry and, as can be seen in Fig. 8, the spectra of the pairs ^{210,216}Pb and ^{212,214}Pb are predicted to be identical to all orders of perturbation theory, if only two-body interactions are considered. Within a single-j approach with two- and three-body interactions, only the latter break particle-hole symmetry. In Subsect. 6.1 it was shown that a three-body interaction, fit to data, is indeed capable of reproducing the evolution of spectra with mass number A. Here we find that the effective two-plus-three-body interaction, which we derived from the Kuo-Herling interaction in the shell-model space consisting of the 82–126 neutron orbitals and calculated up to third order, does not have the correct behavior. As seen from the upper panel in Fig. 8, its effect on the energies goes in the wrong direction since the Th_{2+3} spectrum compresses with increasing mass number A. Only when the exact effective two-plus-three-body interaction is taken does one reproduce the experimental trend, as seen from the lower panel in Fig. 8.

Results concerning $E2$ transitions in the even Pb isotopes are shown in Table 5. The second column of the table lists the $B(E2)$ values for the various transitions as obtained with an effective two-body interaction calculated up to third order and with a standard one-body $E2$ operator. In the third and fourth columns are given the $B(E2)$ values

obtained with an additional two-body piece of the $E2$ operator, calculated up first and second order, respectively. The fifth column lists the most complete results when the effect of the three-body interaction calculated up to third order is taken into account. The sixth column, labeled 'SM", gives the results of the shell model in the full space. The seventh column, labeled 'Exp', lists the measured $B(E2)$ values—those in ^{210}Pb taken from Ref. [20] and the $B(E2; 8^+ \to 6^+)$ values in the other isotopes estimated from Ref. [23]. All calculated $B(E2)$ values are obtained with a constant length of the harmonic oscillator, $b = 2.456$ fm, and an effective neutron charge $e_\nu = 0.77$, which is fixed from the $B(E2; 2^+ \to 0^+)$ value in ^{210}Pb.

At present the sequence of decays $8^+ \to 6^+ \to 4^+ \to 2^+ \to 0^+$ is measured only in ^{210}Pb and the $B(E2)$ values have rather large error bars. If the $E2$ data in ^{210}Pb turn out to be confirmed with smaller error bars, this would be not so much a problem of the effective operators but rather one of the Kuo-Herling interaction in the full space, akin to what is found in ^{210}Po [28]. The results of Table 5 demonstrate that the two-body piece of the effective $E2$ operator, calculated to first order, provides an important correction to the $B(E2)$ values while the contribution of the second-order term is only minor. The three-body interaction has an important effect on the $B(E2)$ values in ^{212}Pb and an equally important but opposite effect in ^{214}Pb. Note that three-body interaction has no influence on the $B(E2)$ values in the two-particle or two-hole isotopes ^{210,216}Pb, as the structure of the states is independent of the interaction, at least in a single-orbital approach.

The overall conclusion that can be drawn from Table 5 is that the final calculated $B(E2)$ values result from a delicate balance of possibly conflicting effects of an effective three-body interaction and an effective two-body $E2$ operator. Given also the difficulty in reproducing the observed $B(E2)$ values in the two-particle nucleus ^{210}Pb, it seems therefore that conclusions regarding higher-order operators are difficult to draw at this point.

7. Summary and conclusions

We presented the results of a shell-model study of Hamiltonians with two- and three-body interactions and of transition operators with up to two-body terms. We limited ourselves to nuclei where valence nucleons of one kind (i.e., either neutrons or protons) occupy dominantly a single-j orbital such as $0g_{9/2}$ or $1g_{9/2}$, in particular, the $N = 50$ isotones and the lead ($Z = 82$) isotopes.

In the first part of this study we found that the three-body interaction is important to obtain an improved description of excitation spectra of semi-magic nuclei. We argued that the clearest evidence for the presence of effective higher-body forces in nuclei can be obtained from the properties of spectra rather than from binding energies. Such evidence, in particular the breaking of particle-hole symmetry, exists in the $N = 50$ isotones and the lead isotopes, and we found that a three-body interaction can adequately reproduce the experimental trends. The separate components of the

three-body interaction, however, could not be determined reliably from an empirical fit: A small variation in the input data was seen to lead to large fluctuations in the three-body matrix elements.

In the second part of this study we constructed, based on the perturbation theory, an effective single-j Hamiltonian with up to three-body interactions and an effective electric quadrupole operator with up to two-body terms. The validity of the perturbation approach was verified by comparing results obtained with effective operators in a single-j orbital with those obtained in the full shell-model space. Convergence to the shell-model energy spectra in the full space was checked by increasing the order of the interaction (up to three-body) and by increasing the order of perturbation theory (up to third order). Likewise, $E2$ transition probabilities were obtained with a single-j operator with up to two-body terms, calculated up to third order in perturbation theory, and compared to results obtained in the full shell model.

Concerning the effective Hamiltonian, formulas indicate that it is obtained from an expansion in $V/\Delta\epsilon$, the average interaction matrix element over a single-particle energy splitting. We noted that *convergence is slowest for the matrix elements that matter most*, i.e., the two- and three-body pairing matrix elements. Consequently, calculating all matrix elements consistently up to a given order (as one is bound to do), we found that the resulting spectroscopy was poor and that the binding energies were not well reproduced. In particular, the breaking of particle-hole symmetry—the clearest signature of a higher-body force—was not properly described with an effective two-plus-three-body Hamiltonian calculated up to third order in perturbation theory.

We also showed results obtained with an 'exact' two-plus-three-body effective interaction. We argued that this exact interaction is equivalent with the one obtained with the Okubo-Lee-Suzuki (OLS) approach under the assumption that a single off-diagonal three-body matrix element can be neglected. Although with the exact two-plus-three-body effective interaction the breaking of particle-hole symmetry was better accounted for and the calculation at least reproduced the trend of the shell-model results in the full space, the description of binding energies was not convincing and no advantage over an exact two-body effective interaction was found. The simplest possible explanation of these failures is that the effective Hamiltonian contains a non-negligible four-body component. As mentioned in the introduction, it is possible to extend the present study to four-body interactions but, given also the uncertainties of a perturbation expansion, it should be done in a OLS approach since off-diagonal matrix elements may play an important part in the analysis.

Finally, as to effective transition operators, we found ourselves confronted with a complex problem of several higher-order contributions of different origin, which may or may not act constructively. It seems to us that it will be difficult to reach any firm conclusion with regard to three-body interactions in a nucleus solely on the basis of its electromagnetic transition properties.

Acknowledgement

We would like to thank M Rejmund for his expert help with the large-scale shell-model calculation.

References

[1] H-W Hammer, A Nogga and A Schwenk, *Rev Mod Phys* **85** (2013) 197
[2] R B Wiringa and S C Pieper, *Phys Rev Lett* **89** (2002) 182501
[3] B R Barrett, P Navrátil and J P Vary, *Prog Part Nucl Phys* **69** (2013) 131
[4] A Poves and A Zuker, *Phys Reports* **70** (1981) 235
[5] J Sinatkas, L D Skouras, D Strottman and J D Vergados, *J Phys G: Nucl Part Phys* **18** (1992) 1377
[6] L Coraggio, A Covello, A Gargano and N Itaco, *Phys Rev C* **80** (2009) 044311
[7] M Nomura, *Phys Lett B* **40** (1972) 522
[8] C Bloch and J Horowitz, *Nucl Phys* **8** (1958) 91
[9] J N Ginocchio and J B French, *Phys Lett* **7** (1963) 137
[10] J D McCullen, B F Bayman and L Zamick, *Phys Rev* **134** (1964) B515
[11] C Quesne, *Phys Lett B* **31** (1970) 7
[12] I Eisenstein and M W Kirson, *Phys Lett B* **47** (1973) 315
[13] A Volya, *Eur Phys Lett* **86** (2009) 52001
[14] P Van Isacker and I Talmi, *Eur Phys Lett* **90** (2010) 32001
[15] A de-Shalit and I Talmi, *Nuclear Shell Theory* (Academic Press, New York, 1963)
[16] I Talmi, *Simple Models of Complex Nuclei. The Shell Model and Interacting Boson Model* (Harwood, Academic, Chur, Switzerland, 1993)
[17] G Racah, *Phys Rev* **76** (1949) 1352
[18] I Talmi, *Phys Rev Lett* **107** (1957) 326
[19] W J Huang, G Audi, M Wang, F G Kondev, S Naimi and X Xu, *Chin Phys C* **41** (2017) 030002
[20] National Nuclear Data Center, http://www.nndc.bnl.gov
[21] W J Mills *et al.*, *Phys Rev C* **75** (2007) 047302
[22] J Jolie, private communication
[23] A Gottardo *et al. Phys Rev Lett* **109** (2012) 162502
[24] A F Lisetskiy, B A Brown, M Horoi and H Grawe, *Phys Rev C* **70** (2004) 044314
[25] T T S Kuo and G H Herling, US Naval Research Laboratory Report nr 2258 (1971)
[26] G H Herling and T T S Kuo, *Nucl Phys A* **181** (1972) 113
[27] H Mach *et al.*, *Phys Rev C* **95** (2017) 014313
[28] D Kocheva *et al.*, *Eur Phys J A* **53** (2017) 175
[29] P Van Isacker, unpublished
[30] S Okubo, *Prog Theor Phys* **12** (1954) 603
[31] K Suzuki and S Y Lee, *Prog Theor Phys* **64** (1980) 2091
[32] T Otsuka, T Suzuki, J D Holt, A Schwenk and Y Akaishi, *Phys Rev Lett* **105** (2010) 032501

Appendix A. Energies of the two-nucleon state

In this appendix we give the expressions for the energy of the two-nucleon state $|j^2 J\rangle$ in second- and third-order perturbation theory. We introduce a short-hand notation for the different matrix elements that enter the subsequent expressions,

$$V_k^J \equiv \langle j^2 J|\hat{V}_2|jj_kJ\rangle, \quad V_{kl}^J \equiv \langle j^2 J|\hat{V}_2|j_kj_lJ\rangle, \quad V_{k,k'}^J \equiv \langle jj_kJ|\hat{V}_2|jj_{k'}J\rangle,$$

$$V^J_{k,k'l'} \equiv \langle j j_k J|\hat{V}_2|j_{k'} j_{l'} J\rangle, \quad V^J_{kl,k'l'} \equiv \langle j_k j_l J|\hat{V}_2|j_{k'} j_{l'} J\rangle, \tag{A.1}$$

and similarly for the energy differences,

$$\Delta\epsilon_k \equiv \epsilon_j - \epsilon_{j_k}, \quad \Delta\epsilon_{kl} \equiv 2\epsilon_j - \epsilon_{j_k} - \epsilon_{j_l}. \tag{A.2}$$

By straightforward application of stationary perturbation theory, the second-order contribution of $\hat{V}_2$ to the energy of the state $|j^2 J\rangle$ is

$$E^{(2)}(j^2 J) = \sum_k \frac{|V^J_k|^2}{\Delta\epsilon_k} + \sum_{k\le l} \frac{|V^J_{kl}|^2}{\Delta\epsilon_{kl}}, \tag{A.3}$$

and the third-order contribution equals

$$\begin{aligned} E^{(3)}(j^2 J) = &\sum_k \sum_{k'} \frac{V^J_k V^J_{k,k'} V^J_{k'}}{\Delta\epsilon_k \Delta\epsilon_{k'}} + \sum_{k\le l} \sum_{k'\le l'} \frac{V^J_{kl} V^J_{kl,k'l'} V^J_{k'l'}}{\Delta\epsilon_{kl}\Delta\epsilon_{k'l'}} \\ &+ 2\sum_k \sum_{k'\le l'} \frac{V^J_k V^J_{k,k'l'} V^J_{k'l'}}{\Delta\epsilon_k \Delta\epsilon_{k'l'}} - V_J \left(\sum_k \frac{|V^J_k|^2}{(\Delta\epsilon_k)^2} + \sum_{k\le l} \frac{|V^J_{kl}|^2}{(\Delta\epsilon_{kl})^2} \right). \end{aligned} \tag{A.4}$$

Appendix B. Energies of the three-nucleon state

In this appendix we give the expressions for the energy of the three-nucleon state $|j^3 \alpha J\rangle$ in second- and third-order perturbation theory. The former is given by

$$E^{(2)}(j^3 \alpha J) = \sum_{k,L} \frac{|V^J_{kL}|^2}{\Delta\epsilon_k} + \sum_{k\le l,L} \frac{|V^J_{klL}|^2}{\Delta\epsilon_{kl}}, \tag{B.1}$$

which contains the following three-particle matrix elements:

$$\begin{aligned} V^J_{kL} &\equiv \langle j^3 \alpha J|\hat{V}_2|j^2(L) j_k J\rangle \\ &= \sqrt{6}(-)^{j-j_k}[L] \sum_R [R] c^R_{3\alpha J} \begin{Bmatrix} j & R & J \\ j_k & L & j \end{Bmatrix} V^R_k, \end{aligned} \tag{B.2}$$

$$V^J_{klL} \equiv \langle j^3 \alpha J|\hat{V}_2|j_k j_l(L) j J\rangle = \sqrt{3} c^L_{3\alpha J} V^L_{kl}. \tag{B.3}$$

With use of the expressions (A.3) and (B.1) in the general expansion (12) it can be shown that the effective three-body interaction to second order reduces to [14]

$$\langle j^3 \alpha J|\hat{V}^{(2)}_{3\text{eff}}|j^3 \alpha J\rangle = 3 \sum_k \sum_{RR'} [R][R'] c^R_{3\alpha J} c^{R'}_{3\alpha J} \begin{Bmatrix} j & J & R \\ j & j_k & R' \end{Bmatrix} \frac{V^R_k V^{R'}_k}{\Delta\epsilon_k}, \tag{B.4}$$

which does not contain any contribution from the $|j_k j_l(L) j J\rangle$ configurations. The energy of the three-nucleon state $|j^3 \alpha J\rangle$ in third-order perturbation theory is given by

$$\begin{aligned} E^{(3)}(j^3 \alpha J) = &\sum_{k,L} \sum_{k',L'} \frac{V^J_{kL} V^J_{kL,k'L'} V^J_{k'L'}}{\Delta\epsilon_k \Delta\epsilon_{k'}} + \sum_{k\le l,L} \sum_{k'\le l',L'} \frac{V^J_{klL} V^J_{klL,k'l'L'} V^J_{k'l'L'}}{\Delta\epsilon_{kl}\Delta\epsilon_{k'l'}} \\ &+ 2\sum_{k,L} \sum_{k'\le l',L'} \frac{V^J_{kL} V^J_{kL,k'l'L'} V^J_{k'l'L'}}{\Delta\epsilon_k \Delta\epsilon_{k'l'}} \\ &- V_{j^3\alpha J} \left(\sum_{k,L} \frac{|V^J_{kL}|^2}{(\Delta\epsilon_k)^2} + \sum_{k\le l,L} \frac{|V^J_{klL}|^2}{(\Delta\epsilon_{kl})^2} \right), \end{aligned} \tag{B.5}$$

which contains, besides (B.2) and (B.3), the three-particle matrix elements

$$V_{j^3\alpha J} \equiv \langle j^3\alpha J|\hat{V}_2|j^3\alpha J\rangle = 3\sum_R (c^R_{3\alpha J})^2 V_R, \tag{B.6}$$

$$\begin{aligned} V^J_{kL,k'L'} &\equiv \langle j^2(L)j_kJ|\hat{V}_2|j^2(L')j_{k'}J\rangle \\ &= V_L\delta_{LL'}\delta_{kk'} + 2(-)^{j_k-j_{k'}}[L][L'] \\ &\quad\times\sum_R [R]^2 \begin{Bmatrix} j & j & L \\ J & j_k & R\end{Bmatrix}\begin{Bmatrix} j & j & L' \\ J & j_{k'} & R\end{Bmatrix} V^R_{k,k'}, \end{aligned} \tag{B.7}$$

$$\begin{aligned} V^J_{klL,k'l'L'} &\equiv \langle j_kj_l(L)jJ|\hat{V}_2|j_{k'}j_{l'}(L')jJ\rangle \\ &= V^L_{kl,k'l'}\delta_{LL'} + [L][L']\hat{P}(j_kj_lL)\hat{P}(j_{k'}j_{l'}L') \\ &\quad\times\sum_R [R]^2 \begin{Bmatrix} j_l & j_k & L \\ J & j & R\end{Bmatrix}\begin{Bmatrix} j_{l'} & j_{k'} & L' \\ J & j & R\end{Bmatrix} V^R_{l,l'}\delta_{kk'}, \end{aligned} \tag{B.8}$$

$$\begin{aligned} V^J_{kL,k'l'L'} &\equiv \langle j^2(L)j_kJ|\hat{V}_2|j_{k'}j_{l'}(L')jJ\rangle \\ &= [L][L']\hat{P}(j_{k'}j_{l'}L')\begin{Bmatrix} j_{l'} & j_{k'} & L' \\ J & j & L\end{Bmatrix} V^L_{l'}\delta_{kk'} \\ &\quad - \sqrt{2}(-)^{j+j_k+L'}[L][L']\begin{Bmatrix} j & j & L \\ J & j_k & L'\end{Bmatrix} V^{L'}_{k,k'l'}, \end{aligned} \tag{B.9}$$

where $\hat{P}$ is the exchange operator defined by

$$\hat{P}(jj'J)f(j,j',J) = \frac{f(j,j',J) - (-)^{j+j'-J}f(j',j,J)}{\sqrt{1+\delta_{jj'}}}, \tag{B.10}$$

for any function $f(j,j',J)$ of the angular momenta j, j', and J.

Appendix C. Effective two-body transition operator

In this appendix we give the expressions for the effective two-body transition operator in first- and second-order perturbation theory. These can be obtained from the general expression (16) together with the eigenstates of $\hat{H}_1 + \hat{V}_2$ up to second order

$$|j^2J)^{(1+2)} \approx (1+s^J)|j^2J\rangle + \sum_k (f^J_k + s^J_k)|jj_kJ\rangle + \sum_{k\le l}(f^J_{kl} + s^J_{kl})|j_kj_lJ\rangle, \tag{C.1}$$

with coefficients f of the first order in $V/\Delta\epsilon$

$$f^J_k = \frac{V^J_k}{\Delta\epsilon_k}, \quad f^J_{kl} = \frac{V^J_{kl}}{\Delta\epsilon_{kl}}, \tag{C.2}$$

and coefficients s of the second order in $V/\Delta\epsilon$

$$\begin{aligned} s^J &= -\frac{1}{2}\left(\sum_k \frac{|V^J_k|^2}{(\Delta\epsilon_k)^2} + \sum_{k\le l}\frac{|V^J_{kl}|^2}{(\Delta\epsilon_{kl})^2}\right), \\ s^J_k &= \sum_{k'}\frac{V^J_{k,k'}V^J_{k'}}{\Delta\epsilon_k\Delta\epsilon_{k'}} + \sum_{k'\le l'}\frac{V^J_{k,k'l'}V^J_{k'l'}}{\Delta\epsilon_k\Delta\epsilon_{k'l'}} - \frac{V^JV^J_k}{(\Delta\epsilon_k)^2}, \\ s^J_{kl} &= \sum_{k'}\frac{V^J_{kl,k'}V^J_{k'}}{\Delta\epsilon_{kl}\Delta\epsilon_{k'}} + \sum_{k'\le l'}\frac{V^J_{kl,k'l'}V^J_{k'l'}}{\Delta\epsilon_{kl}\Delta\epsilon_{k'l'}} - \frac{V^JV^J_{kl}}{(\Delta\epsilon_{kl})^2}. \end{aligned} \tag{C.3}$$

For example, the effective two-body transitions operator to first order equals

$$\langle j^2 J_{\rm f}\|\hat{T}^{(1)}_{\rm 2eff}\|j^2 J_{\rm i}\rangle = \sum_k \frac{V_k^{J_{\rm i}}}{\Delta\epsilon_k}\langle j^2 J_{\rm f}\|\hat{T}_1\|jj_k J_{\rm i}\rangle + \sum_k \frac{V_k^{J_{\rm f}}}{\Delta\epsilon_k}\langle jj_k J_{\rm f}\|\hat{T}_1\|j^2 J_{\rm i}\rangle, \quad \text{(C.4)}$$

in terms of the matrix elements V_k^J and energy differences $\Delta\epsilon_k$ defined in Appendix A.

Let us specify to the case of most interest here, namely an electric one-body operator of the form

$$\hat{T}_{1,\mu}(\lambda) = e\sum_i r_i^\lambda Y_{\lambda\mu}(\theta_i,\phi_i), \quad \text{(C.5)}$$

with e the effective charge of the nucleon. The expression (C.4) then reduces to

$$\begin{aligned}\langle j^2 J_{\rm f}\|\hat{T}^{(1)}_{\rm 2eff}(\lambda)\|j^2 J_{\rm i}\rangle = e(-)^{j+1/2+\lambda}\sqrt{2}[j][J_{\rm i}][\lambda][J_{\rm f}]\sum_k [j_k]\begin{pmatrix} j & \lambda & j_k \\ -\frac{1}{2} & 0 & \frac{1}{2}\end{pmatrix} \\ \times\left(\frac{V_k^{J_{\rm i}}}{\Delta\epsilon_k}\begin{Bmatrix} j & j_k & \lambda \\ J_{\rm i} & J_{\rm f} & j\end{Bmatrix} + \frac{V_k^{J_{\rm f}}}{\Delta\epsilon_k}\begin{Bmatrix} j & j_k & \lambda \\ J_{\rm f} & J_{\rm i} & j\end{Bmatrix}\right) I^\lambda_{n\ell n_k\ell_k}, \quad \text{(C.6)}\end{aligned}$$

with the radial integral

$$I^\lambda_{n\ell n'\ell'} = \frac{1}{\sqrt{4\pi}}\int_0^{+\infty} r^\lambda R_{n\ell}(r)R_{n'\ell'}(r)r^2 dr, \quad \text{(C.7)}$$

where it is assumed that $(-)^{\lambda+\ell+\ell'} = +1$.

With use of the expansion (C.1) the second-order two-body components of an effective transition operator are

$$\begin{aligned}\langle j^2 J_{\rm f}\|\hat{T}^{(2)}_{\rm 2eff}(\lambda)\|j^2 J_{\rm i}\rangle = (s^{J_{\rm i}} + s^{J_{\rm f}})\langle j^2 J_{\rm f}\|\hat{T}_1(\lambda)\|j^2 J_{\rm i}\rangle \\ + \sum_k s_k^{J_{\rm i}}\langle j^2 J_{\rm f}\|\hat{T}_1(\lambda)\|jj_k J_{\rm i}\rangle \\ + \sum_{k'} s_{k'}^{J_{\rm f}}\langle jj_{k'} J_{\rm f}\|\hat{T}_1(\lambda)\|j^2 J_{\rm i}\rangle \\ + \sum_k\sum_{k'} f_k^{J_{\rm i}} f_{k'}^{J_{\rm f}}\langle jj_{k'} J_{\rm f}\|\hat{T}_1(\lambda)\|jj_k J_{\rm i}\rangle \\ + \sum_k\sum_{k'\le l'} f_k^{J_{\rm i}} f_{k'l'}^{J_{\rm f}}\langle j_{k'}j_{l'} J_{\rm f}\|\hat{T}_1(\lambda)\|jj_k J_{\rm i}\rangle \\ + \sum_{k\le l}\sum_{k'} f_{kl}^{J_{\rm i}} f_{k'}^{J_{\rm f}}\langle jj_{k'} J_{\rm f}\|\hat{T}_1(\lambda)\|j_k j_l J_{\rm i}\rangle \\ + \sum_{k\le l}\sum_{k'\le l'} f_{kl}^{J_{\rm i}} f_{k'l'}^{J_{\rm f}}\langle j_{k'}j_{l'} J_{\rm f}\|\hat{T}_1(\lambda)\|j_k j_l J_{\rm i}\rangle, \quad \text{(C.8)}\end{aligned}$$

where, for an electric transition operator, the one-body matrix elements are

$$\begin{aligned}\langle j_a j_b J_{\rm f}\|r^\lambda Y_\lambda\|j_c j_d J_{\rm i}\rangle = \hat{P}(j_a j_b J_{\rm f})\hat{P}(j_c j_d J_{\rm i})(-)^{j_c+\frac{1}{2}+\lambda+J_{\rm f}}[J_{\rm i}][J_{\rm f}][\lambda][j_b][j_d] \\ \times\begin{Bmatrix} j_b & j_d & \lambda \\ J_{\rm i} & J_{\rm f} & j_a\end{Bmatrix}\begin{pmatrix} j_b & \lambda & j_d \\ -\frac{1}{2} & 0 & \frac{1}{2}\end{pmatrix} I^\lambda_{n_b\ell_b n_d\ell_d}\delta_{ac}. \quad \text{(C.9)}\end{aligned}$$